

# Manufacture of Ultrahigh-Modulus Poly(oxymethylenes) by Die Drawing

P. S. HOPE,\* A. RICHARDSON, and I. M. WARD, *Department of Physics, University of Leeds, Leeds LS2 9JT, England*

## Synopsis

A stable experimental die drawing process has been operated for poly(oxymethylene) over a range of temperature. Rods possessing room-temperature Young's moduli up to 23 GPa were produced using a homopolymer grade, the values obtained from a copolymer being somewhat lower. This compares favorably with the best modulus achieved by hydrostatic extrusion but is rather lower than that produced by conventional drawing; reasons for this are discussed. A stable die drawing process has also been operated for glass fiber-reinforced poly(oxymethylene), but extensive macroscopic void formation occurred in the products under all conditions, reducing their potential for practical application.

## INTRODUCTION

In recent years, techniques for the production of ultrahigh-modulus oriented polymers have been investigated by many workers. In our laboratories, efforts have concentrated on solid-phase forming methods, such as drawing and hydrostatic extrusion, at elevated temperatures. While most attention has been paid to linear polyethylene (LPE), from which the most significant modulus enhancement was obtained, two other polymers, polypropylene (PP) and poly(oxymethylene) (POM), have also been examined; and more modest, but still very useful, improvements in modulus have been reported.

Tensile drawing has been studied on an experimental scale using conventional tensile testing machines for LPE,<sup>1,2</sup> PP,<sup>3,4</sup> and POM,<sup>5</sup> and a continuous process has been developed for the production of high-modulus fibers and tapes. The major limitation on such a process is its inability to produce samples with diameters (or thicknesses) much greater than 0.5 mm. This can be overcome by the use of hydrostatic extrusion, in which a billet of solid polymer is forced to flow through a conical, converging die by the action of a fluid at high pressure. LPE,<sup>6-10</sup> PP,<sup>11</sup> and POM<sup>12</sup> have also been examined by this technique, and a variety of product sections, including circular, square, and I-section rod, sheet, and tube, have been produced in a range of sizes up to 60 mm.

One penalty incurred by the production of such large sections is a reduction in the maximum degree of deformation, and hence product modulus, that can be achieved. There are several reasons for this. The strain and strain rate paths followed by material in a conical die are less favorable than those experienced during free tensile drawing, and the flow stress of the polymer consequently increases substantially toward the die exit. The flow stress in hydrostatic extrusion is further increased by the high levels of hydrostatic pressure, and there is a

\* Present address: B. P. Chemicals Limited, Sully, Penarth, South Glamorgan, CF6 2YU, England.

significant amount of friction between the billet and die, which can also be shown to increase the required extrusion pressures. Finally, at higher product thicknesses, there is the possibility of adiabatic extrusion, which can lead to process instability. A quantitative analysis of the mechanics of the hydrostatic extrusion process for polymers (valid for stable, isothermal process conditions) has been published elsewhere.<sup>13,14</sup>

The die drawing process, which was first described by Coates and Ward<sup>15</sup> for PP and by Gibson and Ward<sup>16</sup> for LPE, is a technique which combines the best features of free tensile drawing and hydrostatic extrusion, enabling large section products to be made at the high-modulus levels obtainable by free drawing. The process, shown schematically in Figure 1, is similar to wire drawing in that a billet of solid polymer is drawn through a heated conical die solely by the action of a haul-off force applied to the product, but differs in that the polymer leaves the wall of the die before the die exit. This is of crucial importance, as the polymer is then able to follow a more favorable strain and strain rate path, reducing the required flow stress. Friction is also lowered because of the diminished area of contact between billet and die. A second and equally important advantage over hydrostatic extrusion is the absence of a significant hydrostatic pressure in the die, which reduces material flow stress levels.

The degree of deformation imparted to the material by the process is characterized by the actual draw ratio ( $R_A$ ), defined as the ratio of the billet cross-sectional area to that of the product. Because the polymer draws away from the die wall during the process,  $R_A$  is always greater than the nominal draw ratio ( $R_N$ ), which is defined as the ratio of the billet cross-sectional area to that of the die exit. Deformation can be considered to take place in three distinct zones (Fig. 1). In zone I, the polymer remains in contact with the die and therefore remains at the die temperature. In zone II, the polymer is no longer in contact with the die wall, but should nevertheless remain substantially at the die temperature. Outside the die, the temperature of the material falls to ambient over a finite distance, the polymer meanwhile continuing to draw down until a constant product diameter is reached, at which point the limit of deformation zone III is defined.

Clearly, the exact positions of the boundaries between zones are difficult to define in practice. In particular, the position at which the polymer separates from the die wall depends on the value of  $R_N$ , the die temperature, and the im-

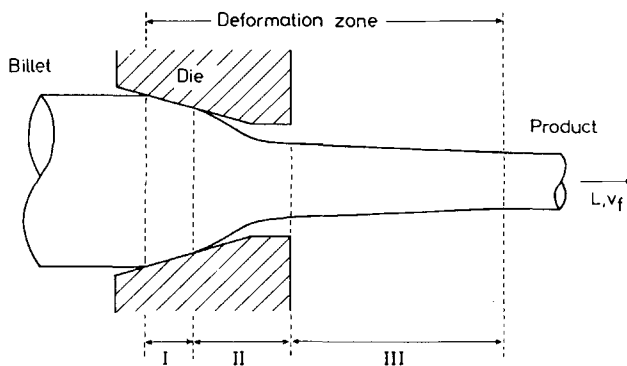


Fig. 1. Schematic diagram of die drawing process.

posed haul-off velocity; hence a number of routes to a given draw ratio are possible, as is discussed later. The position of the end of zone III (where deformation ceases) is determined by a complex relationship between the strain-hardening behavior and the temperature sensitivity of the polymer.

As well as being able to produce larger-diameter LPE and PP samples with moduli equal to those of the highest-modulus drawn fibers, the process has the additional advantage of operating at high production rates. The capital cost of equipment for commercial exploitation is low compared to solid-phase extrusion techniques, and a continuous process may readily be envisaged.<sup>15-17</sup> However, although the process has been operated in a stable manner for rod, multifilament, and tube,<sup>17</sup> it is possible that limitations in terms of product stability may arise for noncircular sections.

Following the successful application of the process to LPE and PP, the purpose of the present work is to assess its practical value as a method of manufacturing ultrahigh-modulus POM. POM is considered a particularly promising polymer for conversion to ultrahigh-modulus components, because of the relatively good properties of the isotropic polymer, which is known to exhibit better stiffness, creep resistance, fatigue endurance, and temperature stability than most other engineering thermoplastics. As well as commercially available homopolymer and copolymer grades, a short glass fiber-reinforced copolymer grade is examined.

## EXPERIMENTAL

### Materials and Billet Preparation

Details of the materials used for the investigation are given in Table I. These were chosen to allow a comparison between homopolymer and copolymer and to examine the effect of glass fiber filling. All three grades are available commercially in bar stock form and have similar values of weight-average molecular weight ( $\bar{M}_w \sim 10^5$ ) and melt flow index (MFI in the region 2.5-5.0). Previous experience in drawing<sup>5</sup> and hydrostatic extrusion<sup>12</sup> of POM has shown this MFI range to be suitable for solid-phase processing.

Cylindrical billets for die drawing were produced by machining from bar stock. The billet diameter was chosen to give the required nominal draw ratio ( $R_N$ ) for a die exit-bore diameter ( $d_f$ ) of 4 mm. A tag of length 20 mm, followed by a tapered nose cone of semiangle  $5^\circ$ , was turned on each billet in order to allow gripping and to assist the starting procedure for the process.

TABLE I  
POM Grades Used for Die Drawing

| Manufacturer | Code   | Type                                                          | Melting point, °C <sup>a</sup> |
|--------------|--------|---------------------------------------------------------------|--------------------------------|
| du Pont      | D500   | homopolymer                                                   | 176                            |
| Celanese     | M25-01 | copolymer                                                     | 165                            |
| Celanese     | GC-20  | copolymer containing 20%<br>(by weight) short<br>glass fibers | 165                            |

<sup>a</sup> Measured by differential scanning calorimetry at a heating rate of 10°C/min.

### Die Drawing Experiments

Die drawing was performed on an Instron tensile testing machine, using the apparatus shown in Figure 2. A steel die was held within a temperature-controlled aluminum block, and the system was calibrated (using a dummy billet containing a thermocouple) so that the temperature of the material in the die could be prescribed to  $\pm 1^\circ\text{C}$ . The die used for all experiments was conical, with a semiangle of  $15^\circ$ ; the bore diameter at the die exit and the land length were both 4 mm.

During drawing, the Instron was operated at constant crosshead speed, and the draw load ( $L$ ) was monitored by means of a load cell in series with the apparatus. Before each run, a billet was placed within the heated block so that the tag protruded through the die, and the (self-gripping) draw grips were attached. The assembly was then allowed to reach thermal equilibrium at the prescribed nominal billet temperature ( $T_N$ ), which normally took approximately 30 min. The drawing process was then started at a low crosshead speed ( $v_f$ ), usually in the region of 10 mm/min. In a typical run, the draw load increased gradually until a steady value was reached, the onset of which corresponded to the point where all the material in the starting cone of the billet had been drawn through the die. After this point, the diameter of the drawn material produced was found to be stable, and the process was considered to have reached steady-state conditions.

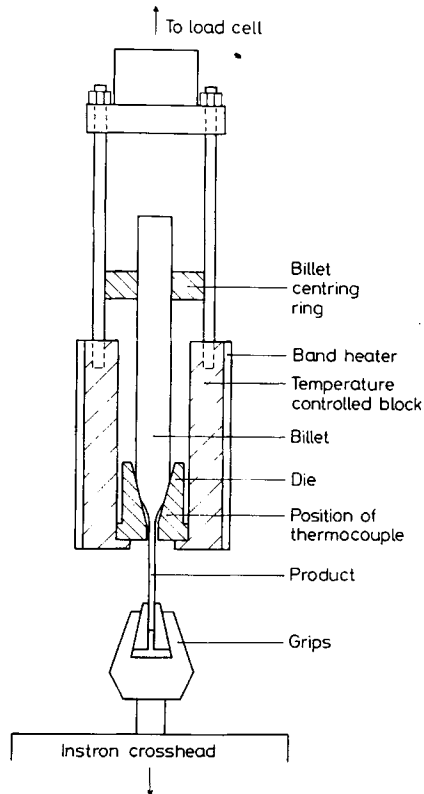


Fig. 2. Experimental die drawing apparatus.

In order to investigate the effect of draw speed on the deformation ratio attained and the draw load required, it was necessary to increase  $v_f$  several times during each run. Following a step increase in  $v_f$ , the load generally rose quite steadily until a new stable load was reached, corresponding to a different set of steady-state conditions. This procedure was repeated until a limiting draw speed was reached, at which the product fractured, for each nominal draw ratio.

If at any time during the process the step change in draw speed was large, then the draw load rose rapidly and passed through a peak, after which it fell before continuing to rise again more slowly to its steady-state value. This load peak, the height of which increased with the size of the draw speed increment, was similar to that sometimes observed following yield in conventional drawing of polymers. In die drawing, the peak is thought to arise as a result of necking in the product, and indeed for sufficiently large speed increments, fracture of the product occurred. This phenomenon effectively limited both the speed at which draw could be initiated and the rate at which the draw speed could be increased during the process. A programmed gradual increase in draw speed would therefore be desirable during the start-up procedure for a commercial die drawing process.

### Stiffness Measurements

The isochronous (10 s) Young's modulus was measured for each drawn sample at 20°C, using a dead-loading three-point bend test. This type of test was preferred to tensile tests because of the simplicity of the apparatus, the increased measuring accuracy (due to the large deflection for a given strain), and the fact that no sample gripping damage is caused. Care was taken to ensure that all measurements were performed at strain levels below  $10^{-3}$ , and high sample length/diameter ratios were maintained to minimize end effects.<sup>18</sup>

It should be noted that the presented modulus results are not corrected for the possible presence of voids within the samples.

### Density Measurements

The densities of the products were measured by means of the density bottle technique, with water as the fluid. By weighing the samples both before and after immersion, it was possible to correct for any fluid uptake by voids.

### Scanning Electron Microscopy

Scanning electron microscopy (SEM) studies were performed on a Cambridge stereoscan 150 Mk.2 instrument, using samples produced by razor blade slicing at room temperature.

## RESULTS

### Processing Behavior

In previous studies of the tensile drawing behavior of POM homopolymers, both Clark and Scott<sup>19</sup> and Brew and Ward<sup>5</sup> found the optimum draw temperature to be in the region of 150°C. For hydrostatic extrusion, Coates and Ward<sup>12</sup>

found 164°C to be satisfactory for POM homopolymers, while Hope and Ward<sup>20</sup> have found 150°C to be suitable for copolymers. Therefore, to investigate the effect of die temperature (having regard to the nonisothermal nature of the die drawing process as operated here), initial experiments were performed on the copolymer grade at nominal temperatures of 135, 150, and 158°C. The results are shown in Figure 3, where the actual draw ratios of the products and the required draw loads are plotted as functions of draw speed. All the data presented are for good-quality, stable products.

As reported previously for the die drawing of LPE and PP,<sup>15,16</sup> the most notable feature of the results is the increase in  $R_A$  with draw speed. At all temperatures, this increase is approximately linear for draw speeds below 100 mm/min, above which the curves diverge. At lower values of  $R_N$ , the curves tend to level out at higher draw speeds, while for higher values of  $R_N$  (i.e., larger-diameter starting billets), there are signs of an upturn in  $R_A$  with draw speed, in which case the process terminates by product fracture at draw ratios in the region of 10 to 15. Fracture always occurred following the formation of a localized neck in the product, just beyond the die exit, and was usually preceded by stress whitening of the necked region.

At all temperatures, the draw load initially increases with draw speed but tends toward a steady value at speeds above 100 mm/min. Gibson and Ward<sup>16</sup> have discussed the mechanism by which the load is stabilized for die drawing of LPE and conclude that the process is self-stabilizing by virtue of the ability of the polymer to leave the die wall at the optimum position. In this way, the work done in the process is minimized, as a result of the change in the balance between the amount of deformation taking place in zones I and II (Fig. 1).

The general form of the relationships in Figure 3, as well as the range of values of  $R_A$  and  $v_f$ , are very similar to those obtained for the die drawing of medium high-molecular-weight LPE ( $\bar{M}_w \sim 3 \times 10^5$ ), and contrast markedly with those

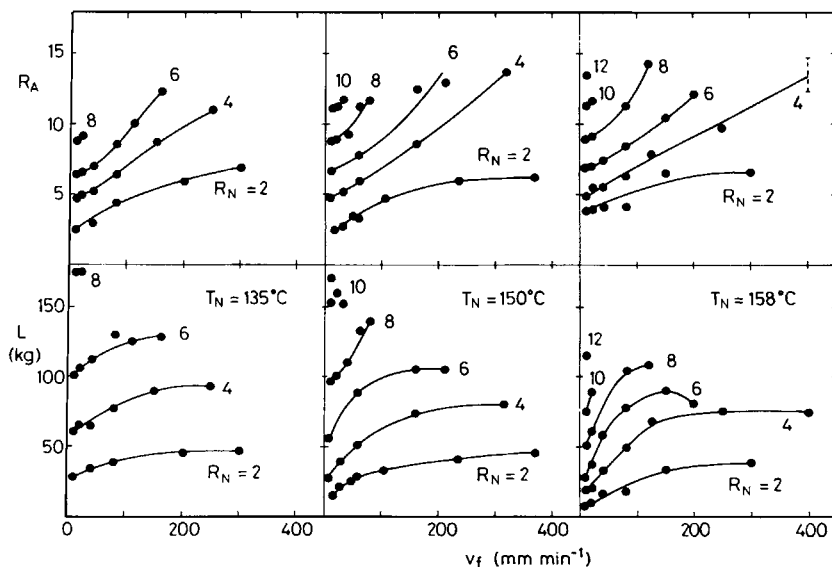


Fig. 3. Variation of draw ratio and draw load with draw speed; copolymer grade M25-01 at various die temperatures.

of low-molecular-weight LPE ( $\bar{M}_w \sim 1 \times 10^5$ ), in which very much higher draw ratios can be achieved but at much lower draw speeds.<sup>16</sup>

The nominal draw temperature has very little effect on the form of the  $R_A$  vs.  $v_f$  relationships. While the maximum value of  $R_N$  which may be drawn successfully increases with draw temperature, there is only a small increase in the actual deformation ratio that can be achieved. However, the draw loads are substantially reduced with increasing temperature, which reflects the decrease in polymer flow stress with temperature.

Figures 4 and 5 show the processing behavior of the homopolymer and the glass fiber-filled copolymer grades, for a nominal draw temperature of 150°C. The behavior of the homopolymer (Fig. 4) is qualitatively very similar to that of the copolymer, although at high draw speeds the actual draw ratio of the  $R_N = 2$  products falls with draw speed. The draw load also falls with draw speed, for  $R_N = 2$  and  $R_N = 4$  at higher speeds. It is not possible at present to identify reasons for these effects, but a buildup of heat in the deforming polymer, similar to that reported for hydrostatic extrusion,<sup>6,8</sup> is one possibility. The draw loads are generally rather higher than those of the copolymer at the same draw temperature but are very similar to those of the copolymer at  $T_N = 135^\circ\text{C}$ , a result which is consistent with the difference in melting point between the grades.

All attempts to increase the draw speed of the glass fiber-filled copolymer above 80 mm/min resulted in fracture of the product beyond the die exit (Fig. 5). Although this type of behavior is quite different from that of the unfilled polymers, the maximum draw ratio achieved was still of the same order ( $R_A \sim 12$ ). The draw loads were generally lower for the glass fiber-filled copolymer.

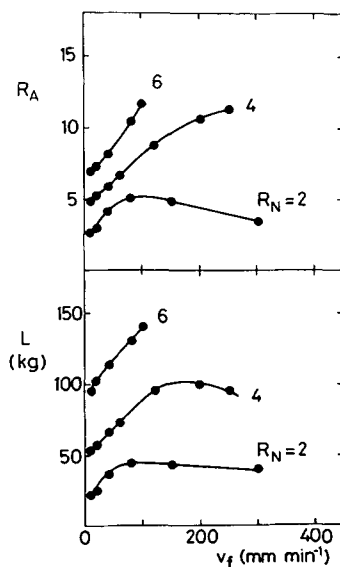


Fig. 4. Variation of draw ratio and draw load with draw speed; homopolymer grade D500,  $T_N = 150^\circ\text{C}$ .

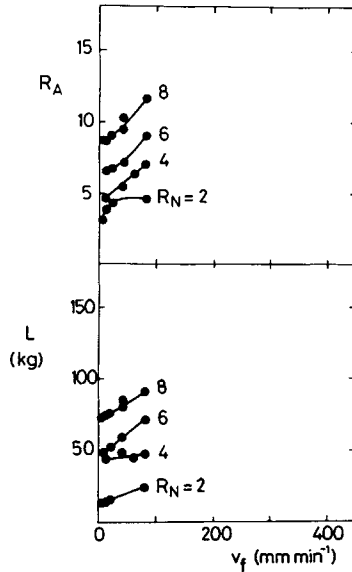


Fig. 5. Variation of draw ratio and draw load with draw speed; glass fiber-filled copolymer grade GC-20,  $T_N = 150^\circ\text{C}$ .

### Product Properties

Visual inspection revealed the surface of the unfilled products to be quite smooth and free from flaws. Both homopolymer and unfilled copolymer products exhibited three types of behavior with increasing draw ratio: in some cases, the products were observed to change from the opaque white of the isotropic material to transparent. This has been seen previously at deformation ratios above 5 for hydrostatically extruded POM<sup>12</sup> and accompanies the transformation from the spherulitic morphology of the isotropic polymer to a fibrillar structure at higher deformation ratios. Sometimes, this transition to transparent material was followed at higher draw ratios by a return to opaque white, while in other cases the material remained opaque white at all draw ratios. This whitening of the products at higher draw ratios, which was observed to occur initially down the core of the samples, has been attributed to the formation of microvoids and is discussed later.

The surface finish of the glass-filled samples was considerably rougher than that of the unfilled polymers, and the products remained opaque at all draw ratios. Both these effects can be attributed to the presence of the glass fibers.

The effect of nominal draw temperature on Young's modulus of the unfilled copolymer is shown in Figure 6. In all cases, the moduli of the products increase more or less linearly with draw ratio, the rate of increase and the maximum modulus value being similar at all temperatures ( $\sim 18$  GPa). While at  $T_N = 135^\circ\text{C}$  the modulus-draw ratio relationship appears to be unique, at temperatures closer to the melting point the data can be separated into a number of distinct curves, each corresponding to a different value of  $R_N$ . This is seen most clearly at  $T_N = 158^\circ\text{C}$ .

Gibson and Ward<sup>16</sup> have pointed out that the moduli obtained from die-drawn LPE are likely to depend on the thermal and strain rate paths followed by the



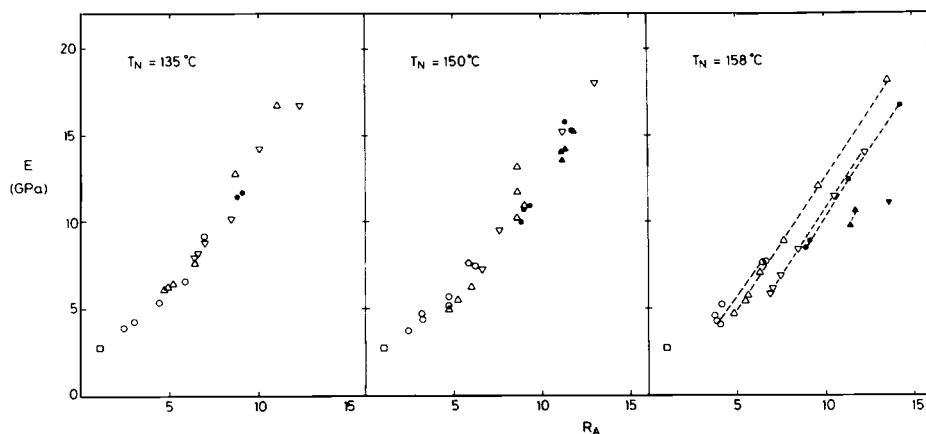


Fig. 6. Variation of product modulus with draw ratio; copolymer grade M25-01 at various draw temperatures ( $\square$ ) isotropic; ( $\circ$ )  $R_N = 2$ ; ( $\Delta$ )  $R_N = 4$ ; ( $\nabla$ )  $R_N = 6$ ; ( $\bullet$ )  $R_N = 8$ ; ( $\blacktriangle$ )  $R_N = 10$ ; ( $\blacktriangledown$ )  $R_N = 12$ .

material after leaving the die. Considering the possible routes to a given value of the actual draw ratio, it is clear from Figures 3–5 that samples drawn from high  $R_N$  billets reach a given value of  $R_A$  at lower draw speeds than those drawn from low  $R_N$  billets. Figure 7 shows three samples removed from the die after drawing to  $R_A = 13$ , from billets with different values of  $R_N$ . Examination of Figure 7 shows that for high  $R_N$  billets (low draw speeds), drawing takes place predominantly within the die (i.e., in zones I and II), and hence predominantly at the nominal draw temperature; while for low  $R_N$  billets (higher draw speeds), substantial drawing occurs beyond the die (i.e., in zone III), and therefore at lower, nonuniform temperatures. The separation of the modulus–draw ratio data into a family of curves is therefore explicable in terms of the increased effectiveness of the drawing process at the lower temperatures of zone III. Such separation is more evident for higher nominal die temperatures, where the temperature fall experienced by the product on leaving the die is larger, resulting in the length of zone III being greater.

This type of behavior contrasts with that observed previously for isothermal plastic deformation processes. For conventional drawn and hydrostatically extruded polymers, unique modulus–draw ratio relationships have been observed

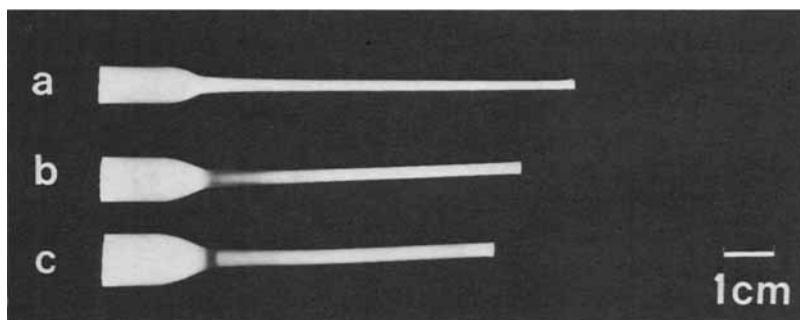


Fig. 7. Samples removed from die after drawing (M25-01,  $T_N = 150^\circ\text{C}$ ). The samples are drawn to the same actual draw ratio ( $R_A = 13$ ) by different routes: (a)  $R_N = 4$ ,  $v_f = 315$  mm/min; (b)  $R_N = 6$ ,  $v_f = 210$  mm/min; (c)  $R_N = 8$ ,  $v_f = 80$  mm/min.

for each grade at a given process temperature. Furthermore, in these materials the product modulus for a given deformation ratio falls with increasing process temperature. Referring to Figure 6, it is perhaps remarkable that for die drawing the highest modulus–draw ratio plots for each  $T_N$  are so similar; the upper limit to the modulus–draw ratio relationship in each case appears to be that at which deformation occurs predominantly in zone III, which suggests that the thermal and strain rate paths followed outside the die are similar for each value of  $T_N$ . In this case, it is interesting to note that the optimum process conditions, in terms not only of product modulus but also of production rate, are those in which the length of zone I is minimized.

The moduli of the homopolymer grades are shown in Figure 8. The slope of the curve is slightly steeper than those of the copolymer grade, with the result that the maximum modulus of 23 GPa is rather higher. Despite the higher modulus of the isotropic billet material, the moduli of the glass-filled copolymer products (Fig. 9) are very similar to those of the unfilled copolymer, the maximum modulus being in the region of 15 GPa. Reasons for this are discussed later.

### Void Formation

The presence of voids in the die-drawn products was suggested by visual examination and confirmed by density measurements and SEM examination. Internal visual examination was only possible for the unfilled products. Voids

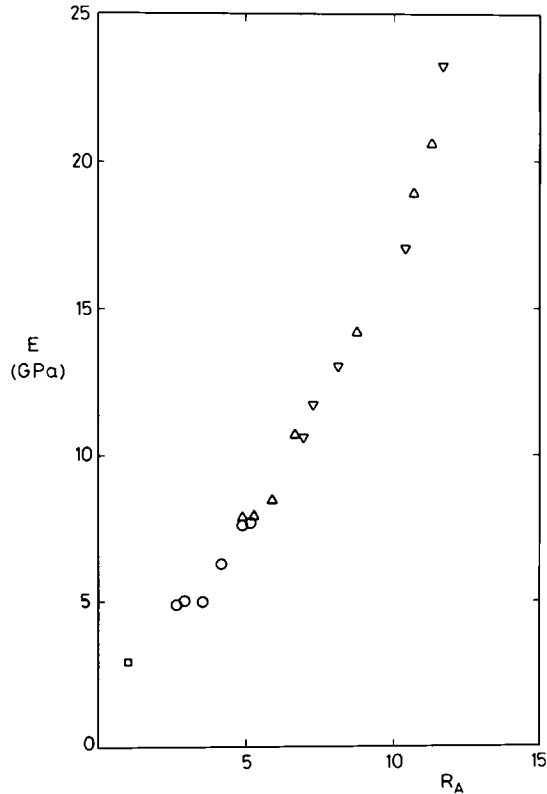


Fig. 8. Variation of product modulus with draw ratio; homopolymer grade D500,  $T_N = 150^\circ\text{C}$ ; (□) isotropic; (○)  $R_N = 2$ ; (△)  $R_N = 4$ ; (▽)  $R_N = 6$ .

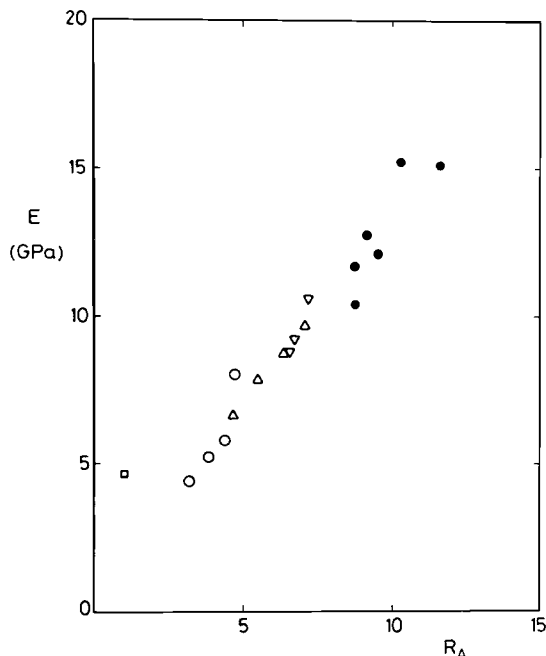
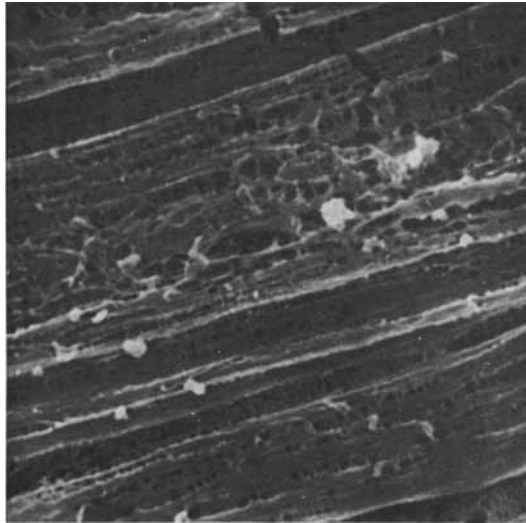


Fig. 9. Variation of product modulus with draw ratio; glass fiber-filled copolymer grade GC-20,  $T_N = 150^\circ\text{C}$ ; ( $\square$ ) isotropic; ( $\circ$ )  $R_N = 2$ ; ( $\Delta$ )  $R_N = 4$ ; ( $\nabla$ )  $R_N = 6$ ; ( $\bullet$ )  $R_N = 8$ .

were observed to form initially along the center line of the products, some short distance beyond the die exit, indicating that voiding occurs during the free drawing part of the process (i.e., in region III). This can be seen in samples (b) and (c) of Figure 7; in sample (a) the voids must have formed before the transformation to a fibrillar structure was complete, and so no transparent region beyond the die is visible.

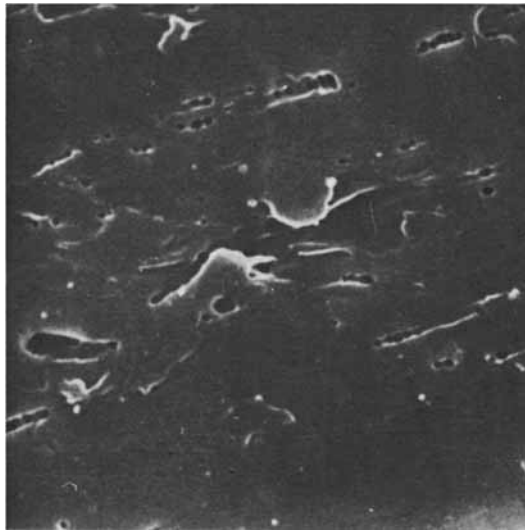
In free tensile drawing of POM,<sup>5</sup> void formation was not observed below draw ratio 12. In die drawing, however, the onset of voiding was observed to occur in some cases at draw ratios as low as 6. This may be simply an effect of scale, as the cross-sectional areas of the die-drawn products were an order of magnitude greater than those of the freely drawn products. If this is so, void formation may prove to be a problem at even lower draw ratios as the process is scaled up to give larger-diameter products.

The occurrence of voids preferentially along the axis of the products was confirmed by SEM studies. Figure 10 shows micrographs of a die-drawn unfilled product of moderate draw ratio. It can be seen immediately that although the voids are similar in type, those at the center of the sample [Fig. 10(a)] occur to a much greater degree than at the edge of the sample [Fig. 10(b)]. The voids appear to form in a "ladder" structure, aligned in the draw direction of the product; close to the center of the sample, the "ladders" appear to be continuous. Microvoids of this type have been reported previously in drawn polymers.<sup>21</sup> A possible explanation of this type of void formation has been proposed by Hookway,<sup>22</sup> who examined voids formed during the cold drawing of nylon 66. Using a theory originally developed by Bridgman<sup>23</sup> to describe the stress distribution at the neck of a tension specimen, the occurrence of voids was shown



5  $\mu$ m

(a)



5  $\mu$ m

(b)

Fig. 10. Scanning electron micrographs of unfilled copolymer grade M25-01,  $R_A = 6.2$ ,  $T_N = 150^\circ\text{C}$ ; longitudinal section: (a) center of sample; (b) edge of sample.

to be consistent with the formation of a negative hydrostatic pressure within the neck. This hydrostatic tension, which is superimposed on the applied draw stress, can be shown to be maximum at the axis of the specimen and zero at the surface, which could account for the dispersion of the voids across the products. Rigorous application of such a theory to explain the voids formed during die

drawing would be extremely difficult, particularly in the present case of a polymer which exhibits a considerable degree of strain hardening and material anisotropy. Nevertheless, the theory is compatible with the experimental observation that no such voids occur during hydrostatic extrusion of POM, where the stress field in the extrusion die is entirely compressive.

Although the opaque nature of the glass-filled products precluded internal visual examination, it was evident from density measurements that voids were present to a much greater degree than in the unfilled polymer (Fig. 11). Calculations based on a three-phase (polymer-fiber-void) model produced void contents of typically 20–40% by volume; but in extreme cases, calculated void contents as high as 69% by volume were observed. This contrasted sharply with the values for unfilled polymer, calculated using a two-phase (polymer void) model, of 4% by volume (average) and 9% by volume (maximum).

Figure 12 shows electron micrographs of a highly voided glass-filled sample. Macroscopic voids can be clearly seen in a micrograph of the whole-product transverse section [Fig. 12(a)], and it is evident that such voids occur to a greater extent close to the sample axis, as was the case for the unfilled product. Figure 12(b) shows that the voids are still large close to the edge of the sample and that the embedded glass fibers appear to be substantially debonded from the polymer matrix.

A longitudinal section close to the center of a similar product [Fig. 13(a)] again shows this macroscopic voiding and debonding, and a high degree of fiber alignment in the draw direction is apparent. At a higher magnification [Fig. 13(b)], the "ladder" structure of microvoids is observed. It is clear, therefore, that in glass-filled die-drawn products there is an extensive formation of macrovoids, superimposed on the microvoid structure of the polymer matrix. It is proposed that these macrovoids are formed as a result of debonding and movement of the glass fibers through the matrix during the drawing process.

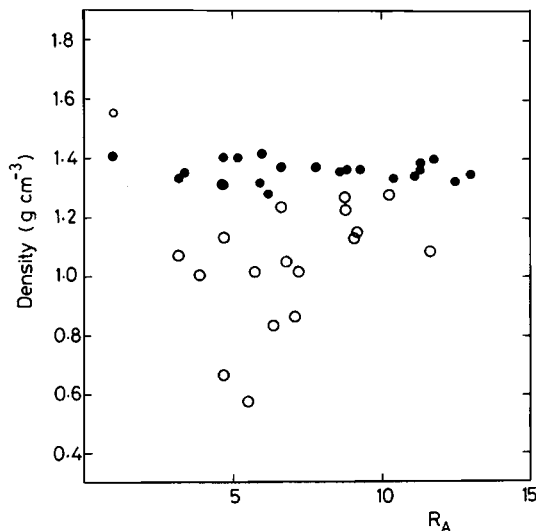
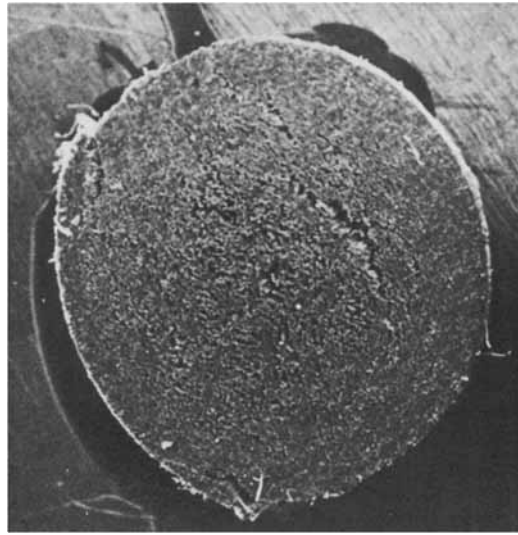
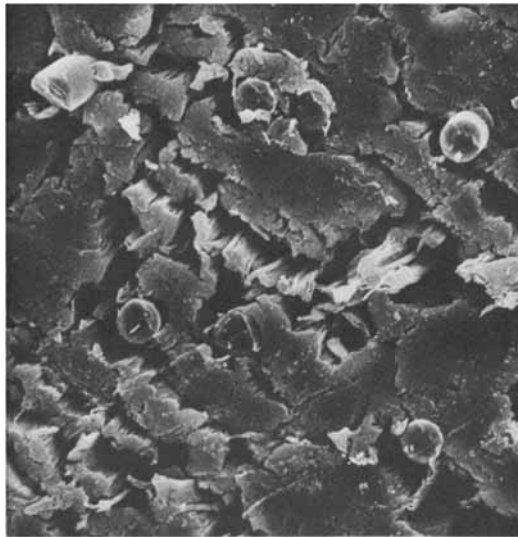


Fig. 11. Product densities for copolymer grades,  $T_N = 150^\circ\text{C}$ : (●) unfilled M25-01; (○) glass-filled GC-20.



(a)

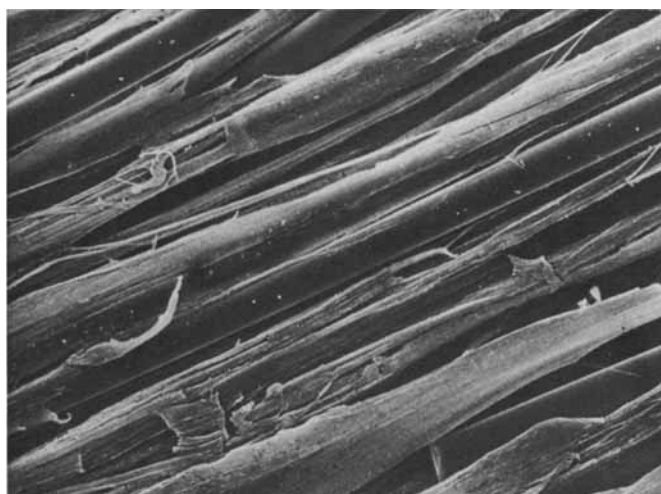


(b)

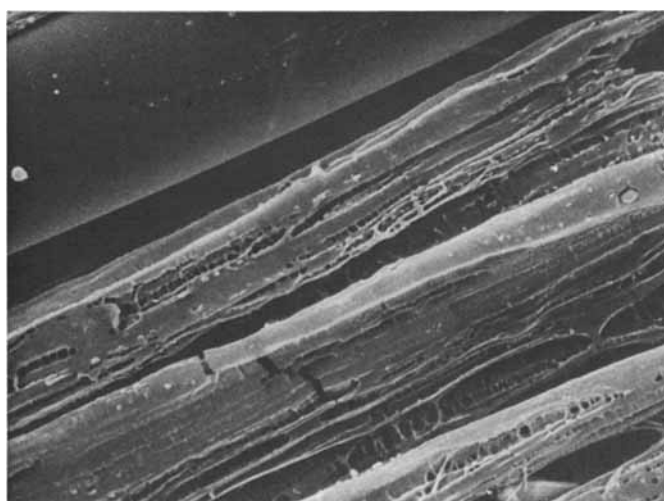
Fig. 12. Scanning electron micrographs of glass-filled copolymer grade GC-20,  $R_A = 5.5$ ,  $T_N = 150^\circ\text{C}$ ; transverse section: (a) whole sample; (b) edge of sample.

## DISCUSSION

Previous publications have reported the maximum degree of deformation (and related modulus) obtained by die drawing LPE<sup>16</sup> and PP<sup>15</sup> to be comparable to that obtained by free tensile drawing and much greater than that obtained by hydrostatic extrusion. The improved performance over hydrostatic extrusion



(a)



(b)

Fig. 13. Scanning electron micrographs of glass-filled copolymer grade GC-20,  $R_A = 7.0$ ,  $T_N = 150^\circ\text{C}$ ; longitudinal section: (a) center of sample; (b) same, higher magnification.

may be attributed to the combination of more favorable strain and strain rate fields in the deformation zone and to the absence of hydrostatic pressure, which is known to increase both the flow stress of the deforming material and the friction between the polymer and the die.

Although these considerations also apply to the die drawing of POM, it is clear that the highest modulus obtained (23 GPa) is considerably lower than the highest reported moduli for free drawing (35–40 GPa).<sup>5,19</sup> It is, however, com-

parable to the highest reported modulus for hydrostatic extrusion (24 GPa).<sup>12</sup> The inability of die drawing to produce materials with the highest moduli may arise as a result of the relatively narrow range of temperature and strain rate necessary for optimization of the drawing process for POM. Brew and Ward<sup>5</sup> have suggested that these stringent conditions for effective draw (i.e., draw producing optimum molecular alignment, and hence stiffness) imply the need for a coincidence between the rates at which specific deformation processes operate in the crystalline and amorphous regions of the polymer. This is consistent with our current views on the deformation behavior of other crystalline polymers, but it appears that the "window" of strain rates and temperatures in which such favorable conditions occur is very much smaller for POM than for LPE and PP.

In die drawing, it is difficult to obtain drawing within the optimum "window" of strain rate and temperature for a number of reasons. Firstly, the strain rate is nonuniform and depends on both the geometry of the die and the draw speed. For a given nominal draw ratio, the draw speed also determines the actual draw ratio achieved; it is therefore only possible to obtain a desired value of  $R_A$  within a desired range of strain rates by careful choice of the appropriate value of  $R_N$ . As the optimum strain rate for effective draw is reported to be very low, it would be necessary to choose a large value of  $R_N$ , very close indeed to the required  $R_A$ . Secondly, under normal process conditions, the temperature varies considerably along the deformation zone. For isothermal drawing, it would again be necessary to choose a low draw speed, with  $R_N \simeq R_A$ , to ensure deformation entirely within zones I and II. While such a procedure would ensure adequate control of strain rate and temperature, the required draw speeds are so small as to be beyond the range of our experiments and of no technological interest.

Practical advantages of die drawing POM are therefore limited to those related to the equipment, namely, low capital cost, low energy consumption, and the viability of a continuous process. Nevertheless, even at relatively modest improvements of stiffness, die-drawn POM may prove of technological value by virtue of its higher temperature stability and superior creep properties in comparison to LPE and PP.

The die drawing behavior of glass-filled POM was clearly dominated by the very high degree of void formation. It is assumed that void formation accounts for both the product fracture at a limiting (rather low) draw speed and the lower observed draw loads for a given area reduction. The effective cross-sectional area of polymer in the product is reduced by the presence of both debonded glass fibers and voids, leading to the requirement for lower loads to give comparable draw stresses.

Voids also have an adverse effect on the mechanical properties of the products. It was obvious on handling that the bending and crushing strengths of the glass-filled products were a great deal lower than those of the unfilled products. Calculations based on a "law of mixtures" model<sup>24</sup> for composite stiffness predict that the moduli of the filled products should be considerably greater than those of the unfilled products. In fact, it is apparent from comparison of Figures 6 and 9 that the moduli of filled and unfilled products are remarkably similar for a given draw ratio, and so debonding of the fibers from the matrix, as seen in the micrographs of Figures 12 and 13, clearly renders the fibers inactive as a reinforcing phase.



This is not the case for hydrostatically extruded products. In studies of the hydrostatic extrusion process for glass-filled POM, to be reported separately,<sup>20</sup> the moduli of the products were found to be considerably greater than those of unfilled extrudates; furthermore, the degree of orientation of the glass fibers was found to increase with deformation ratio, implying that the fibers became fully aligned with the deformation direction at relatively modest degrees of deformation and that negligible debonding of the fibers occurred. The ability to retain a good bond in hydrostatic extrusion must be due to the presence of a totally compressive hydrostatic stress field in the extrusion die.

Die-drawn products of glass-filled POM therefore appear to offer no mechanical property advantages over unfilled POM and appear to have poorer mechanical properties than hydrostatically extruded glass-filled POM.

### CONCLUSIONS

Ultrahigh-modulus POM rods up to 4 mm in diameter have been produced by die drawing. Unlike LPE or PP, the maximum product stiffness obtained by die drawing POM is considerably lower than that reported for free tensile drawing but is comparable to the best stiffness obtained by hydrostatic extrusion. The failure to reproduce the highest stiffness levels by die drawing is due to difficulties in achieving the narrow band of temperature and strain rate required to optimize the drawing process for POM. These arise partly because the strain rates required are too low to be of practical interest, but also because of the nonisothermal nature of the process, as a result of which changes in the prescribed die temperature have a relatively small influence on the processing behavior and product properties.

The moduli of the copolymer products were somewhat lower than those of the homopolymer; this effect has been observed previously for drawn, die-drawn, and hydrostatically extruded LPE and may be related to the lower crystallinities (and possibly lower degrees of crystal perfection) in the copolymer products. Some microvoiding was observed, which has been attributed to the presence of a hydrostatic tensile stress in the sample neck during the free-drawing part of the process.

While there are no advantages over hydrostatically extruded POM in terms of stiffness, the inherent advantages of die drawing (potential for a continuous process, low capital costs, and higher production rates) make the process technologically attractive, particularly in view of the creep and thermal properties of POM, which are superior to those of LPE and PP.

Although a stable die drawing process can be operated for glass fiber-filled POM, debonding of the fibers from the polymer matrix, accompanied by extensive macroscopic void formation, cause the glass-filled products to be of less practical interest than the unfilled products.

The authors wish to thank Dr. M. G. Dobb of the Textile Physics Laboratory, Department of Textile Industries, University of Leeds, for his assistance with the SEM studies. During the course of this work, P.S.H. was supported by a grant from the Celanese Research Company, and A.R. was supported by the Science Research Council.

### References

1. G. Capaccio, T. A. Crompton, and I. M. Ward, *J. Polym. Sci. Polym. Phys. Ed.*, **14**, 1641 (1976).
2. G. Capaccio, T. A. Crompton, and I. M. Ward, *J. Polym. Sci. Polym. Phys. Ed.*, **18**, 301 (1980).
3. D. L. M. Cansfield, G. Capaccio, and I. M. Ward, *Polym. Eng. Sci.*, **16**, 721 (1976).
4. A. J. Wills, G. Capaccio, and I. M. Ward, *J. Polym. Sci. Polym. Phys. Ed.*, **18**, 493 (1980).
5. B. Brew and I. M. Ward, *Polymer*, **19**, 1338 (1978).
6. A. G. Gibson and I. M. Ward, *J. Polym. Sci. Polym. Phys. Ed.*, **16**, 2015 (1978).
7. P. S. Hope, A. G. Gibson, B. Parsons, and I. M. Ward, *Polym. Eng. Sci.*, **20**, 540 (1980).
8. P. S. Hope and B. Parsons, *Polym. Eng. Sci.*, **20**, 589 (1980).
9. P. S. Hope and B. Parsons, *Polym. Eng. Sci.*, **20**, 597 (1980).
10. P. S. Hope, A. G. Gibson, and I. M. Ward, *J. Polym. Sci. Polym. Phys. Ed.*, **18**, 1243 (1980).
11. T. Williams, *J. Mater. Sci.*, **8**, 59 (1973).
12. P. D. Coates and I. M. Ward, *J. Polym. Sci. Polym. Phys. Ed.*, **16**, 2031 (1978).
13. P. D. Coates, A. G. Gibson, and I. M. Ward, *J. Mater. Sci.*, **15**, 359 (1980).
14. P. S. Hope and I. M. Ward, *J. Mater. Sci.*, **16**, 1511 (1981).
15. P. D. Coates and I. M. Ward, *Polymer*, **20**, 1553 (1979).
16. A. G. Gibson and I. M. Ward, *J. Mater. Sci.*, **15**, 979 (1980).
17. A. G. Gibson and I. M. Ward, *Polym. Eng. Sci.*, **20**, 1229 (1980).
18. R. G. C. Arridge, P. J. Barham, C. J. Farrell, and A. Keller, *J. Mater. Sci.*, **11**, 788 (1976).
19. E. S. Clark and L. S. Scott, *Polym. Eng. Sci.*, **14**, 682 (1974).
20. P. S. Hope and I. M. Ward, unpublished work.
21. H. Hendus and E. Penzel, *Chemiefas. Textil-Ind.*, **26**, 527 (1976).
22. D. C. Hookway, *J. Text. Inst.*, **49**, 292 (1958).
23. P. W. Bridgman, *Trans. Am. Soc. Metals*, **32**, 553 (1944).
24. H. Krenchel, *Fibre Reinforcement*, Akademisk Forlag, Copenhagen, 1964.

Received November 18, 1980

Accepted February 12, 1981